Journal of Power Sources 195 (2010) 2514–2519

Contents lists available at ScienceDirect

Journal of Power Sources

journal homepage: www.elsevier.com/locate/jpowsour

Au@BICUVOX10 composite cathode for novel structure low-temperature solid-oxide fuel cells

Tao Yang, Fan Li, Dingguo Xia*

College of Environmental & Energy Engineering, Beijing University of Technology (BJUT-CEEE), Chaoyang District 100022, Beijing, China

ARTICLE INFO

Article history:
Received 16 November 2009
Accepted 16 November 2009
Available online 20 November 2009

Keywords:
Cathode
Au nanoparticles
BICUVOX10
Core–shell structure
Low-temperature SOFC

ABSTRACT

A composite Au@$Bi_2Cu_{0.1}V_{0.9}O_{5.35}$ (BICUVOX10) cathode is prepared and tested as a ceramal electrode for use in low-temperature solid-oxide fuel cells (SOFCs). Au powder is coated onto the surface of BICUVOX10 from an aqueous solution of the chloride with $NaBH_4$ as a reductant. The valence of the surface Au is identified as Au(0) by X-ray photoelectron spectroscopy (XPS). The BICUVOX10 substrate is synthesized from V_2O_3, CuO, and Bi_2O_3 and then investigated by field-emission scanning electron microscopy (SEM). The average size of the particles is estimated to be 100 nm after milling with a planetary ball-mill. The core–shell structure of Au@BICUVOX10 is confirmed by transmission electron microscopy (TEM). The two-dimensional coefficient of thermal expansion (CTE) and the conductivities of mixed powders with different proportions of Au is also tested from room temperature to 600 °C. A single fuel cell is fabricated with Au@BICUVOX10 as the cathode, NiO/GDC ($Gd_{0.1}Ce_{0.9}O_{1.95}$) as the supporting anode, and GDC as the electrolyte. The electrochemical performance is tested and the highest power densities of the fuel cell are determined to be 127, 206, 359, 469, and 474 mW cm^{-2} at 450, 500, 525, 550, and 575 °C, respectively. Finally, the stability of the single SOFC is tested, whereupon it is found that its output is maintained for at least the first 20 h.

1. Introduction

Solid-oxide fuel cells (SOFCs) are promising environmentally friendly electrical power sources, which may be run on diverse fuels such as hydrogen and various hydrocarbons. However, their cost must be reduced substantially for successful commercialization of this technology. Significant efforts have been devoted to lowering the operational temperature of SOFCs to 550–800 °C. In this range, the choice of materials can be greatly expanded and the reliability of cell components will also be improved [1–5]. In the 1980s, F. Abraham reported a new group of low-temperature oxygen-ion conducting materials based on bismuth vanadate ($Bi_4V_2O_{11}$) [1]. Several groups researched the cathode $Bi_2Cu_{0.1}V_{0.9}O_{5.35}$ (known as BICUVOX10) and finally achieved power densities as high as 0.44 W cm^{-2} at 550 °C [6–10]. The interfacial polarization resistance between the electrolyte and the cathode increases rapidly and is largely responsible for the low power density of these fuel cells. Accordingly, the electrode microstructure should be optimized to obtain larger three-phase boundaries (TPBs), which can substantially reduce the interfacial polarization resistance. The TPBs are only electrochemically active if electrons, oxygen vacancies or ions, and oxygen gas can be transported to or away from them. Zhao reported a nano-network of a typical cathode material, $Sm_{0.5}Sr_{0.5}CoO_{3-\delta}$ (SSC), for low-temperature SOFC applications [11]. The nano-network consisted of well-connected SSC nanowires, forming straight conducting paths for oxygen and electron conduction. On the other hand, because of the disadvantage of low electronic transference numbers of BICUVOX10, Liu and Xia mixed some silver powder with BICUVOX10, whereupon the silver network increased the electronic conductivity of the cathode part [10]. However, the long-time stability of the power source incorporating silver was not good.

In this work, we have tried to improve the electronic conductivity of the cathode by coating Au nanoparticles onto BICUVOX10 nanoparticles. This was based on previous findings that Au nanoparticles on appropriate carriers can reduce oxygen at low temperatures [12–14]. The Au nanoparticles not only functioned as an electronic network, but also decreased the polarization of the cathodic oxygen reduction reaction. Also, we took advantage of a new electrolyte structure; Au nanoparticles were distributed on the BICUVOX10, and the finger-like electrolyte was extruded to the active cathode, which increased the TPBs of the cathode–electrolyte interface. Such a cathode microstructure showed extremely high performance and good stability.

* Corresponding author. Tel.: +86 10 67396158.
E-mail addresses: yangtaophoenix@yahoo.com.cn (T. Yang), dgxia@bjut.edu.cn (D. Xia).

0378-7753/$ – see front matter © 2009 Elsevier B.V. All rights reserved.
doi:10.1016/j.jpowsour.2009.11.062

2. Experimental

2.1. Synthesis of the samples

BICUVOX10 powder was prepared by means of a solid-state reaction starting from Bi_2O_3, CuO, and V_2O_3, each of which was obtained from Aldrich. Stoichiometric amounts of these oxides were mixed in ethanol and ground in the mortar of a planetary ball-mill for 4 h at 500 rpm. The evenly mixed powder was then fired for 36 h in air at 750 °C and subsequently cooled to 25 °C at a rate of 40 °C h^{-1}. After the reaction, the BICUVOX10 was milled once more and an 800 mesh sieve was used to remove any oversized particles.

The as-synthesized BICUVOX10 powder was dispersed in a 2 M aqueous solution of $AuCl_4$ and then a freshly prepared 0.5 M $NaBH_4$ solution was added dropwise as a reductant. The solution was stirred continuously. By reduction, some Au nanoparticles were deposited onto the surface of the BICUVOX10, and the brown BICUVOX10 powder turned black after the reaction. The powder was then collected by filtration, washed, and then fired in air at 600 °C for 2 h. To enable facile characterization of the CTE and the conductivity, BICUVOX10 powder was also physically mixed with reduced gold particles in order to press a pellet (denoted as Au–BICUVOX10).

2.2. Characterization

The samples were characterized by X-ray diffraction on a Bruker D-8 Advance diffractometer using Cu-K_α (λ = 1.5405 Å) radiation. The morphology was observed using a Jeol JSM-6500F SEM. The microstructure of the nanoparticles was investigated with the aid of a Jeol MCL J-2010 TEM with an accelerating voltage of 200 kV. TEM samples were prepared by dispersing particles suspended in isopropyl alcohol onto a 3 mm diameter copper grid substrate covered with a porous carbon film. The bulk composition of the ceramal was analyzed by ICP-AES on an IRIS Intrepid spectrometer after dissolution in aqua regia and diluting with 1 M HCl.

XPS measurements were carried out with an X-ray photoelectron spectrometer (Physical Electronics PHI Quantera SXM) using an Al-K_α monochromatic source ($h\nu$ = 1486.6 eV). All binding energies were corrected by taking the principal peak of the carbonaceous matrix at 284.8 eV as an internal standard. The spectra were subsequently analyzed using XPSPEAK 4.1 software.

The CTEs of the Au–BICUVOX10 were measured using a pushrod dilatometer (Netzsch model DIL 402 E) with a quartz standard. All samples were cut into bars 30 mm in length, and the measurements were made in air. The heating/cooling rate was 10 °C min^{-1}.

Electrochemical performances (IM6e, Zahner) of the single fuel cell were characterized from 450 to 575 °C with hydrogen as fuel and air as oxidant at a flow rate of 80 mL min^{-1}. Lifetime tests on the cells were performed at a constant output voltage of 0.5 V. The open-circuit voltage (OCV) in the lifetime tests was recorded separately. The current–voltage curves were obtained in galvanostat mode and electrochemical impedance spectra were measured under open-circuit conditions in the frequency range from 0.1 Hz to 1 MHz.

2.3. Fabrication of the cells

The cells were fabricated by the anode-support method. NiO/GDC ($Ce_{0.9}Gd_{0.1}O_{1.95}$ with 60 wt% NiO) powder was pressed uniaxially into small round pieces of diameter 2.0 cm and the GDC electrolyte was dry-pressed onto the anode together with pore-making carbon powder to form "finger-shaped" microstructures. The pressed electrolyte was then fired at 1350 °C for 5 h. The Au@BICUVOX10 and Au–BICUVOX10 (the molar ratio of Au:BICUVOX10 was 2.5:1, the same as that of the Au@BICUVOX10) composites were brush-painted and fired at 600 °C for 4 h on the half-cells with the help of a screen to ensure that the thickness of the cathode was about 20 μm. The diameter of the cathode was 1.2 cm (area 1.13 cm^2).

For the half-cell used in electrochemical impedance spectra experiments, GDC was pressed on each side and then pore-making carbon powder mixed with further GDC was added to form the "finger-shaped" microstructure, which was similar to the structure of the electrolyte in the single fuel cell. In this case, however, each side of the electrolyte possessed the "finger-shaped" microstructure. The pressed electrolyte was then fired at 1350 °C for 5 h. Each side of the electrolyte was brushed with the Au@BiCUVOX10 cathode. The thickness of the sandwiched half-cell was 1 mm.

3. Results and discussion

3.1. Microstructure of the particles

The BICUVOX10 particles were coated with nanometer gold particles, as evidenced by the TEM characterization (Fig. 1), and

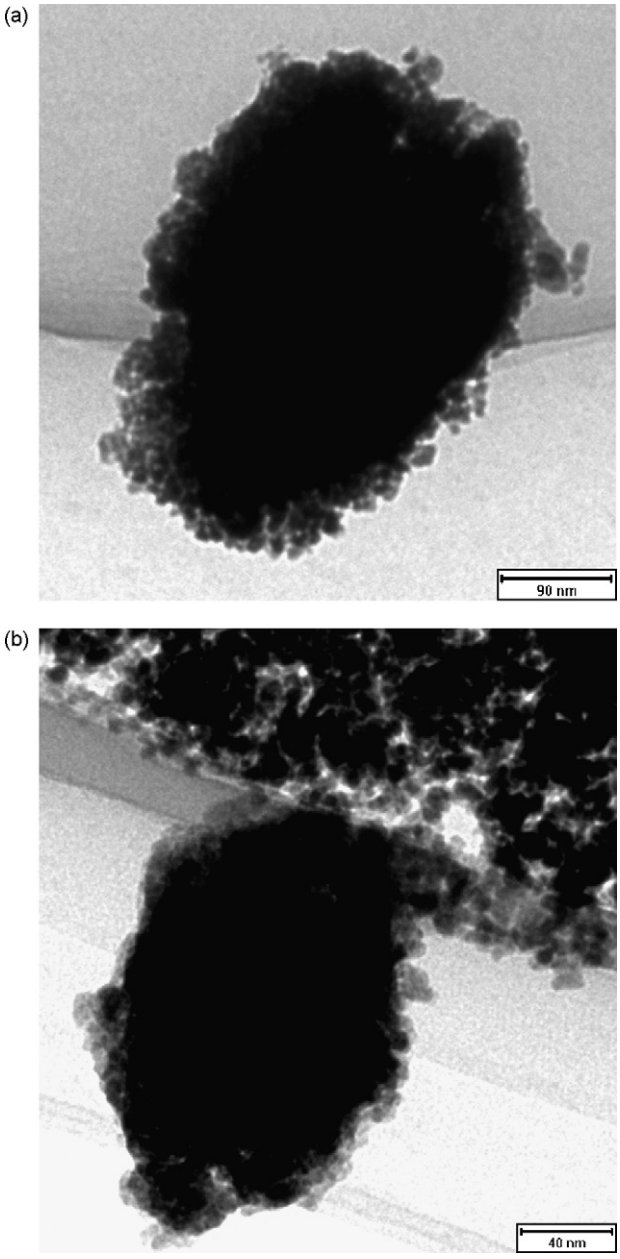

Fig. 1. TEM of BICUVOX10 coated with Au. The bar is 90 nm in (a) and 40 nm in (b).

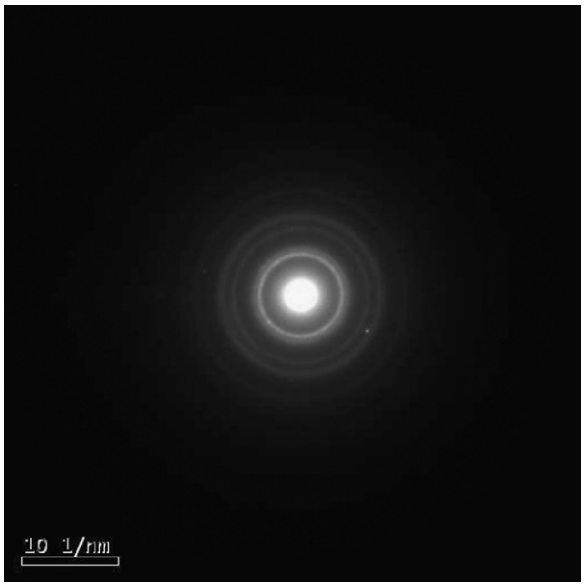

Fig. 2. Selected-area electron diffraction of the edge of the Au@BICUVOX10.

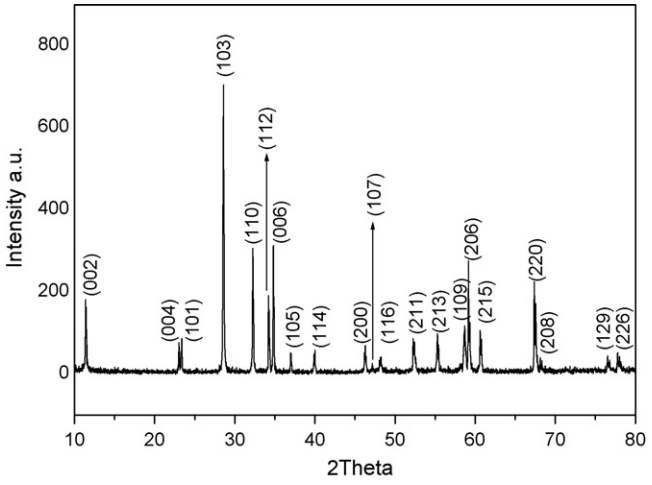

Fig. 3. The XRD profile of BICUVOX10.

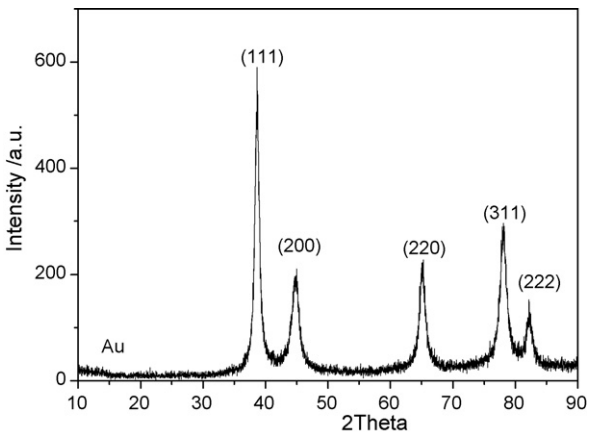

Fig. 4. The XRD profiles of Au. The (1 1 1), (2 0 0), (2 2 0), (3 1 1) and (2 2 2) are the diffraction crystal planes of the fcc Au phase.

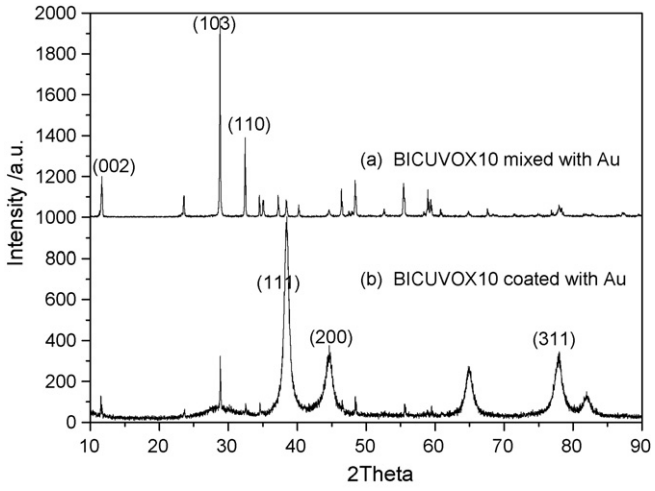

Fig. 5. The XRD profiles of (a) Au–BICUVOX10 and (b) Au@BICUVOX10.

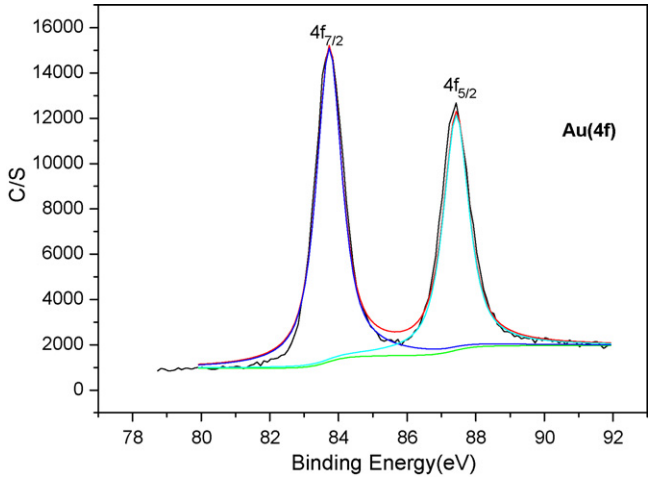

Fig. 6. XPS of Au(4f) of the Au@BICUVOX10.

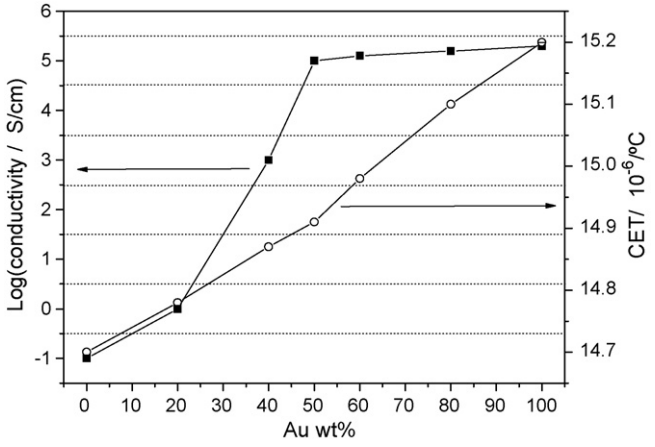

Fig. 7. Profiles of the CTE and the common logarithm of conductivity of the Au–BICUVOX10 with different proportions of Au at 600 °C.

the core BICUVOX10 powder had an average diameter of 90 nm. Gold nanoparticles of diameter approximately 10 nm were evenly coated on the surface of the BICUVOX10, which was evidenced by the selected-area electron diffraction pattern at the edge of the particles (Fig. 2). Besides, many smaller gold particles were also observed (Fig. 1(b)) and the average gold particle size was 10 nm. The extra gold nanoparticles were important for the formation of an electronic conduction network in the process of the cathode preparation.

3.2. XRD characterization

Fig. 3 shows the XRD pattern of the BICUVOX10 synthesized by the solid-state method. The diffraction peaks are in good agreement with the standard Joint Committee on Powder Diffraction Standards (JCPDS) card for BICUVOX10 and no other peaks due to impurities could be detected in the XRD pattern, which confirmed that pure BICUVOX10 could also be obtained using V_2O_3 as a reagent, in place of the pernicious V_2O_5, in the solid-state reaction [6–9]. Fig. 4 shows the XRD pattern of an Au sample. All five peaks can be indexed to the face-centered cubic (fcc) crystalline Au structure, with no other peaks being detected. Fig. 5 shows a comparison of the XRD patterns of BICUVOX10 coated with Au (Au@BICUVOX10) and BICUVOX10 physically mixed with Au (Au–BICUVOX10). In the case of the Au@BICUVOX10 sample, the XRD pattern merely reflects the peaks of the gold particles. This is because almost the entire surface of the BICUVOX10 powder had been covered with Au (as evidenced by TEM), and there

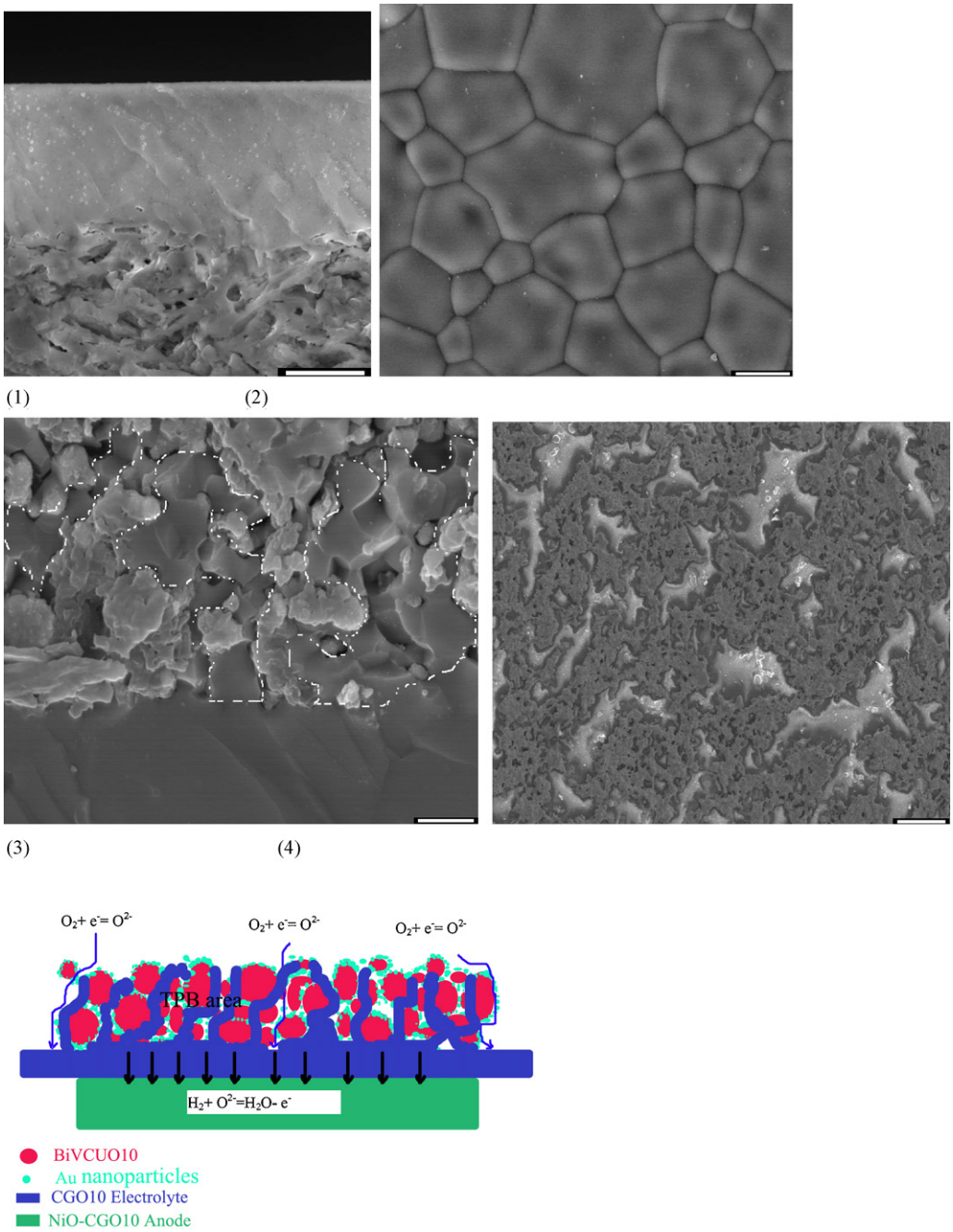

Fig. 8. SEM images of the fuel cells. (1) and (2) are the SEM images of the traditional anode supported half-cell: (1) cross-section image and (2) surface of the cathode. (3) and (4) are the SEM images of the novel structured fuel cell: (3) cross-section image and (4) surface of the cathode. (5) is the schematic diagram of the novel structured fuel cell. The bar is 10 μm in (1), (2), and (3) and 100 μm in (4).

were some spherical gold particles besides the core–shell particles of Au@BICUVOX10. This provided further indirect evidence for the core–shell structure.

For the Au-BICUVOX10 sample, on the other hand, the intensities of the XRD peaks showed similar magnitude because the amounts of Au powder and BICUVOX10 powder exposed to the X-ray beam were at the same level in the mixed powder. The sharp contrast in the XRD results provided further strong evidence of the successful preparation of the core–shell structure of Au@BICUVOX10.

In order to assess the chemical oxidation state of the Au in Au@BICUVOX10, XPS spectra of the sample were acquired. The spectrum of the Au(4f) core level is presented in Fig. 6. The Au4f spectrum shows a doublet comprising a low-energy band ($Au4f^{7/2}$) and a high-energy band ($Au4f^{5/2}$), which could be deconvoluted into a pair of peaks at 83.73 eV and 87.42 eV, respectively. This indicated that the Au was present in only one oxidation state. The absence of a pronounced binding energy shift suggests that the electronic density of Au was the same as that of Au(0) and hence there were no strong electronic interactions between Au and BICUVOX10 in the Au@BICUVOX10 ceramal.

3.3. CTE and conductivity

The two-dimensional CTE and the conductivity of the Au–BICUVOX10 samples with different proportions of Au were tested at up to 600 °C. The CTE and the common logarithm of conductivity ($\log\sigma$) are plotted in Fig. 7. With increasing Au content in the Au–BICUVOX10 samples, the CTE ascended. Theoretically, the CTE of the mixed powder should always be equal to the weighted CTE of each ingredient. Therefore, the CTE profile should be linear throughout the span of compositions ranging from 0% to 100% Au. The experimental CTE value agreed well with the calculated value. However, the conductivity profile was definitely not linear. The conductivity was mainly controlled by the ion migration rate within the BICUVOX10 lattice when the Au content was less than 20%. The ionic conductivity was less than 1 S cm^{-1}. When the percentage of Au was increased to 40%, the conductivity leaped to 1000 S cm^{-1}. A complete conduction network of metal particles was formed within the Au–BICUVOX10 bars when the Au content reached 50%, whereupon the conductivity was controlled almost by the gold itself. From 50% to 100% Au content, the magnitude of the conductivity stayed almost unchanged. The conductivity of pure gold at 600 °C is 1.99×10^5 S cm^{-1}, lower than that at room temperature. Considering the best matching of CTE and conductivity, we suggest that 50 wt% gold is the optimal content. Therefore, Au@BICUVOX10 containing 47 wt% gold was synthesized.

3.4. Microstructure of the single fuel cells

The thickness of the traditional anode was about 1 mm, which supported the whole cell. The electrolyte layer was about 20 μm thick, which was densified by firing, as shown in Fig. 8(1) and (2). Based on reference [15], we improved a novel cathode structure, which is shown in Fig. 8(3), (4), and (5). After deposition onto the surface of the electrolyte and co-firing by the novel method described in Section 2, the finger-like electrolyte was extruded into the active cathode layer. The microstructure of the electrolyte could increase the TPBs of the cathode–electrolyte interface. The average thickness of the cathode layer was controlled to be less than 20 μm. It can clearly be observed from the SEM image that the Au@BICUVOX10 powder was evenly distributed, which was beneficial for the formation of the electronic conducting network within the cathode. The porous cathode permitted the infiltration of oxygen to the TPBs. In addition, the amount of oxygen adsorbed on the metal/ceramic might also have been increased because of the high porosity. The oxygen reduction reaction, which mainly took place at the enlarged TPBs between the Au@BICUVOX10 and electrolyte, could therefore be accelerated. The Au nanoparticles not only functioned as an electronic network, but also decreased the polarization of the cathodic oxygen reduction reaction. This cathodic microstructure showed extremely high performance and good stability.

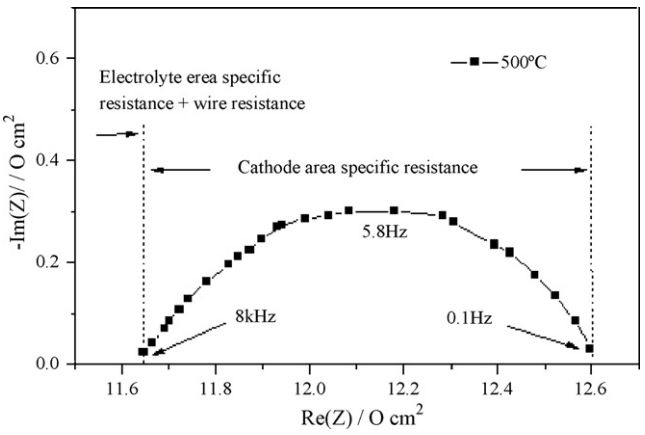

Fig. 9. Electrochemical impedance spectra of the novel structured fuel cell.

3.5. Electrochemical impedance spectra of the novel structured fuel cell

Fig. 9 shows a typical impedance spectrum of the half-cell containing the cathode–electrolyte interface measured at 500 °C. The resistance (about 0.99 Ω cm^2) between the two intercepts with the real axis corresponds to the area-specific resistance (ASR) of the cathode–electrolyte interface [16]. The first intercept with the *x*-axis (11.65 Ω cm^2) is the electrolyte ASR plus the wire resistance. The theoretical electrolyte ASR of GDC of thickness 0.15 cm at 500 °C is 11.61 Ω cm^2 [17]. Our experimentally measured ASR was in good agreement with this value, providing evidence that the electrochemical impedance spectrum was an actual reflection of the cell.

3.6. Specific power density and primal life of the cell

Fig. 10 shows the current–voltage relationships and the calculated power densities of the single fuel cell using Au@BICUVOX10

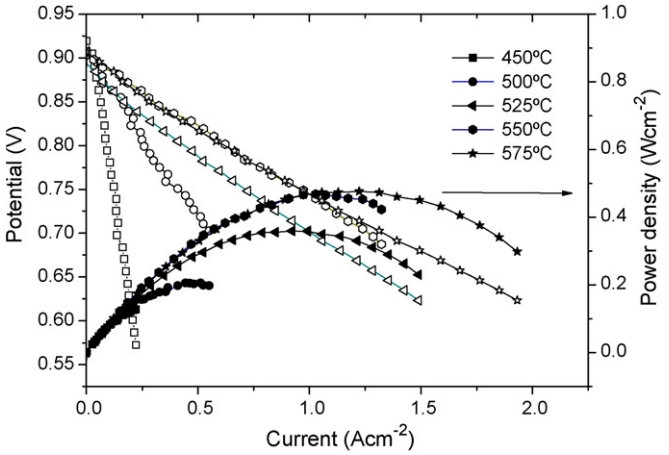

Fig. 10. The *I–V* curves and the corresponding power densities at 450, 500, 525, 550 and 575 °C.

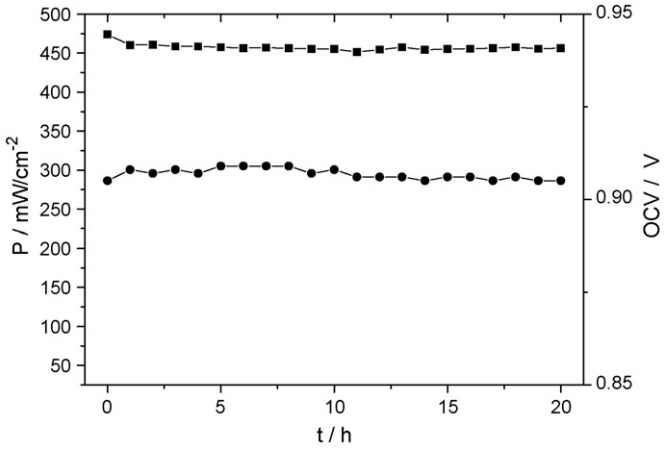

Fig. 11. The OCV and power density profiles in the life test.

as the cathode. The *I–V* data points were recorded after the fuel cell had been stabilized for 20 min. The average OCV of the fuel cell was approximately 0.9 V. The acquired highest power densities of the fuel cell were 127, 206, 359, 469, and 474 mW cm^{-2} at 450, 500, 525, 550, and 575 °C, respectively. For the generic mixed Au–BICUVOX10 cathode, however, the average power densities were 90 mW cm^{-2} lower than that of Au@BICUVOX10 cathode. The results indicated that the electronic network was strengthened and the TPBs were enlarged for the special core–shell structure with the finger-like electrolyte.

The primal long-term stability of the composite cathode, which showed such promising electrochemical properties, was also considered. For the first 20 h, the OCV of the fuel cell was 0.9 V, and the power density was maintained at 450 mW cm^{-2} when the out-circuit voltage was 0.45 V, which was 95% of the initial output (Fig. 11). The results of the electrochemical measurements showed the Au@BICUVOX10 composite to be a potential cathode for use in low-temperature SOFCs. In the low-temperature range, many inexpensive interconnecting and sealing materials that are not amenable to operation at high temperature may be reconsidered. Moreover, the cost of the fabrication techniques could be lowered dramatically.

4. Conclusion

A core–shell Au@BICUVOX10 cathode has been synthesized by chemical reduction and solid-state reactions and assessed for possible use in low-temperature SOFCs. A single fuel cell with a novel finger-like electrolyte has been fabricated using Au@BICUVOX10 as the cathode, NiO/GDC as the anode, and GDC as the electrolyte. This cell successfully generated power densities as high as 474 mW cm^{-2} at 550 °C, and the highest power output was maintained at 95% of its original value for the first 20 h of operation. This assembly technique offers an effective means of improving the efficiency of the cathodic reduction reaction.

Acknowledgements

This work has been supported by the Beijing Natural Science Foundation (Grant No. 207001), the Funding Project for Academic Human Resources Development in Institutions of Higher Learning Under the Jurisdiction of Beijing Municipality, and the National 973 Program of China (Grant No. 2002CB211807). Additional support has been provided by the National Outstanding Youth Fund (Project No. 10125523 to Z.W.).

References

[1] F. Abraham, M.F. Debreuille-Gresse, G. Nowogrochi, Solid State Ionics 28–30 (1988) 529.
[2] B.C.H. Steele, Solid State Ionics 129 (2000) 95.
[3] J.B. Goodenough, A. Manthiram, M. Paranthaman, Y.S. Zhen, Mater. Sci. Eng. B12 (1992) 357.
[4] C.R. Xia, M.L. Liu, Solid State Ionics 144 (2001) 249.
[5] E.P. Murray, S.A. Barnett, Solid State Ionics 143 (2001) 265.
[6] J.C. Boivin, G. Mairesse, Chem. Mater. 10 (1998) 2870–2888.
[7] A.V. Chadwick, C. Colli, C. Maltese, G. Morrison, I. Abrahams, A. Bush, Solid State Ionics 119 (1999) 79.
[8] M. Alga, A. Ammar, R. Essalim, B. Tanouti, F. Mauvy, R. Decourt, Solid State Sci. 7 (2005) 1173.
[9] C.K. Lee, A.R. West, Solid State Ionics 86–88 (1996) 235.
[10] C.R. Xia, M.L. Liu, Adv. Mater. 14 (2002) 521.
[11] F. Zhao, Z.Y. Wang, M.F. Liu, et al., J. Power Sources 185 (1) (2008) 13–18.
[12] G.C. Bond, D.T. Thompson, Gold Bull. 33 (2) (2000) 41–51.
[13] G.C. Bond, D.T. Thompson, Catal. Rev. Sci. Eng. 41 (1999) 319–388.
[14] G.J. Hutchings, M. Haruta, Appl. Catal. A: Gen. 291 (2005) 2–5.
[15] D. Ding, Z.B. Liu, L. Li, C.R. Xia, Electrochem. Commun. 10 (2008) 1295–1298.
[16] Z.P. Shao, S.M. Halle, Nature 43 (2004) 170–173.
[17] H. Inaba, H. Tagawa, Solid State Ionics 83 (1996) 1–16.